Exploring Tubulin-Paclitaxel Binding Modes through Extensive Molecular Dynamics Simulations

Marine Bozdaganyan[1,2], Vladimir Fedorov[2], Ekaterina Kholina[2], Ilya Kovalenko[2], Nikita Gudimchuk[3*], and Philipp Orekhov[1,2,4*]

[1] Faculty of Biology, Shenzhen MSU-BIT University, Shenzhen 518172, China

[2] Faculty of Biology, Lomonosov Moscow State University, Moscow 119234, Russia

[3] Faculty of Physics, Lomonosov Moscow State University, Moscow 119234, Russia

[4] Sechenov University, Moscow 119146, Russia

[*] Correspondence to: ngudimch@gmail.com (N.G.), orekhov_p@smbu.edu.cn (P.O.)

Table S1. Root mean square deviations (RMSD) of the heavy atoms belonging to the binding pocket/paclitaxel calculated between three experimental structures (3j6g, 5syf, and 6ew0) and the structures of clusters 1-5 after roto-translational alignment performed for all residues of the binding site + paclitaxel. Standard deviation is provided where applicable.

	3j6g	***5syf***	***6ew0***	***Cluster 1 (central structure)***	***Cluster 2 (central structure)***	***Cluster 3 (central structure)***	***Cluster 4 (central structure)***	***Cluster 5 (central structure)***
3j6g	0	1.36	1.55	1.90	2.45	2.77	2.82	3.43
5syf	1.36	0	1.46	1.80	2.34	2.43	2.64	3.32
6ew0	1.55	1.46	0	1.78	2.67	2.76	2.79	3.32
Cluster 1	2.11±0.23	2.07±0.23	2.14±0.24	1.93±0.28	2.48±0.15	2.83±0.16	2.70±0.14	3.07±0.16
Cluster 2	2.46±0.23	2.39±0.24	2.61±0.23	2.44±0.26	2.43±0.27	2.82±0.25	2.70±0.14	3.13±0.21
Cluster 3	2.79±0.13	2.47±0.12	2.83±0.12	2.84±0.15	2.97±0.21	1.41±0.29	2.65±0.20	3.50±0.23
Cluster 4	2.81±0.15	2.69±0.15	2.79±0.16	2.68±0.18	2.77±0.14	2.66±0.27	1.9±0.42	2.71±0.21
Cluster 5	3.58±0.14	3.47±0.15	3.51±0.14	3.24±0.13	3.23±0.10	3.49±0.13	2.8±0.15	1.56±0.25

Table S2. Root mean square deviations (RMSD) of the heavy atoms of paclitaxel alone calculated between three experimental structures (3j6g, 5syf, and 6ew0) and the structures of clusters 1-5 after roto-translational alignment performed for all residues of the binding site + paclitaxel. Standard deviation is provided where applicable.

	3j6g	***5syf***	***6ew0***	***Cluster 1 (central structure)***	***Cluster 2 (central structure)***	***Cluster 3 (central structure)***	***Cluster 4 (central structure)***	***Cluster 5 (central structure)***
3j6g	0	1.85	1.31	2.11	4.14	6.80	7.01	9.08
5syf	1.85	0	2.16	2.50	2.71	6.05	6.79	8.63
6ew0	1.31	2.16	0	1.82	4.18	6.88	6.76	8.70
Cluster 1	2.49±0.44	2.82±0.43	2.61±0.49	2.14±0.80	4.75±0.45	6.94±0.33	6.95±0.29	8.40±0.48
Cluster 2	4.41±1.06	3.99±0.99	4.34±1.11	3.97±1.34	4.61±0.80	6.29±0.83	6.75±0.33	7.59±0.73
Cluster 3	6.86±0.17	6.11±0.18	6.91±0.17	7.10±0.17	6.01±0.21	1.22±0.41	6.20±0.12	8.92±0.22
Cluster 4	7.01±0.60	6.76±0.48	6.79±0.60	6.66±0.64	6.69±0.46	6.39±1.03	3.76±1.67	6.45±0.82
Cluster 5	8.90±0.41	8.37±0.39	8.52±0.41	7.98±0.38	8.32±0.37	8.77±0.33	6.48±0.43	2.23±0.99

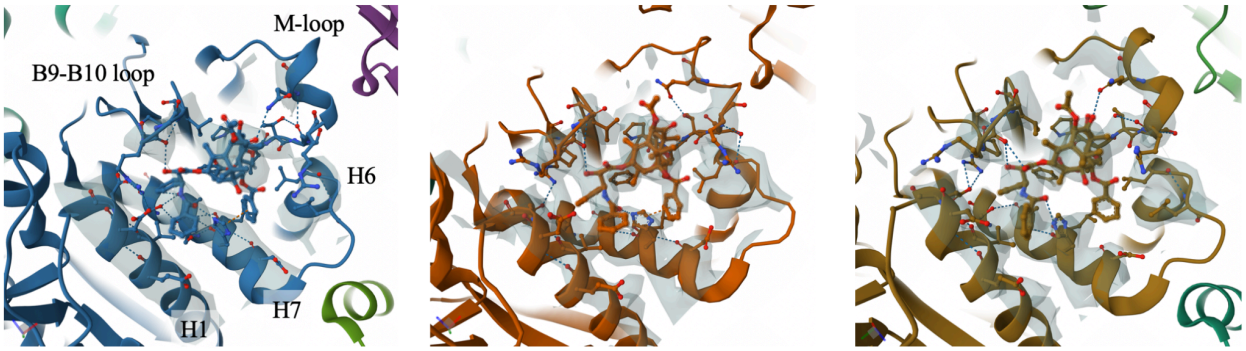

Figure S1. Experimental models of paclitaxel-bound tubulin along with the initial cryoEM densities. Paclitaxel and the neighboring residues are shown using the stick representation. The recommended default density cutoff is used. The images were created using the online Mol* viewer [1].

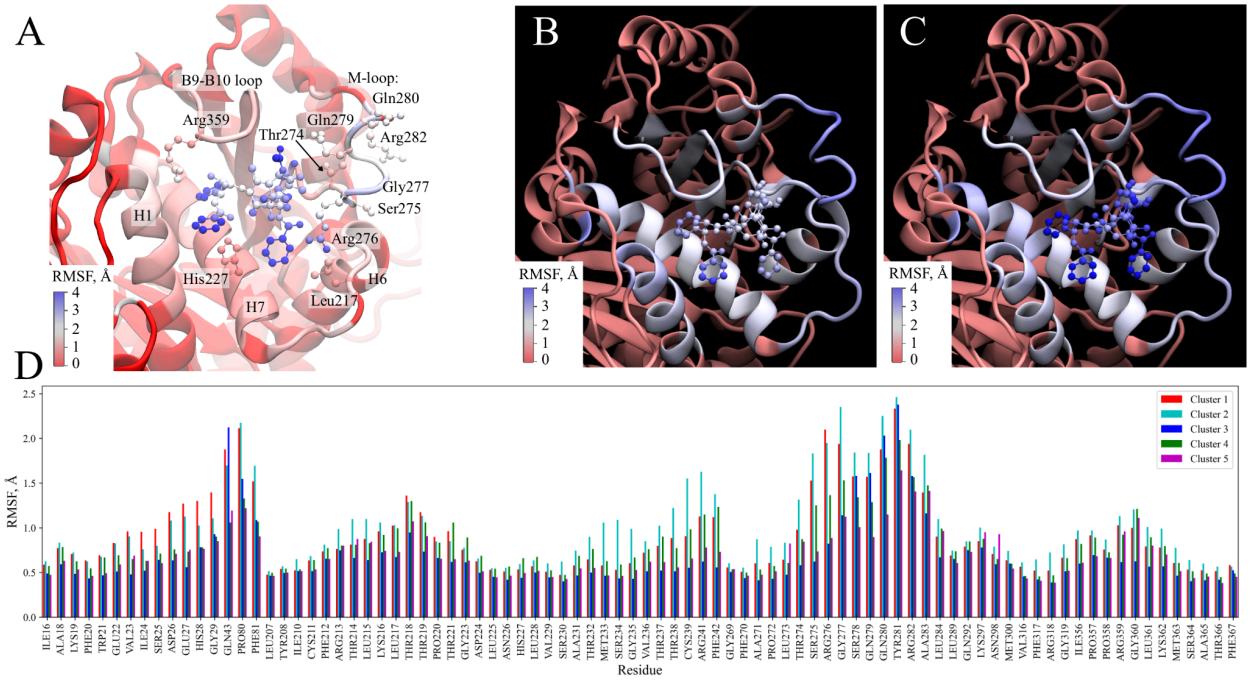

Figure S2. Root mean square fluctuations (RMSF) of atomic positions of paclitaxel in its binding pocket. A-C: paclitaxel and the residues forming its binding site are shown using ball-and-stick (paclitaxel) or stick (amino acids) representation and color-coded according to the atomwise root mean square fluctuations (RMSF) estimated from the full simulated ensemble (panel A), conformations of cluster 1 (panel B), and conformations of cluster 2 (panel C) superimposed using the Cα atoms of the residues belonging to the binding site. The starting conformation of β-tubulin (PDB code 3j6g) is shown using the cartoon representation and colored according to the secondary structure elements. Some key amino acids are captioned. **D:**

Per-residue RMSF estimated for each identified cluster of conformations (1-5) superimposed using the Cα atoms of the residues belonging to the binding site.

Table S3. MM/GBSA binding energies for the clusters of paclitaxel-binding site conformations identified in the simulations and in the experimental structures.

Cluster (1-5) or structure	***Total energy, kcal/mol***			***Contributions, kcal/mol***			
	Mean value	***S.D.***	***Minimal value***	***VdW***	***Electrostatic***	***electrostatic solvation (GB)***	***nonpolar solvation***
1	-11.16	1.95	-16.36	-14.92	-7.90	13.84	-2.18
2	-7.89	1.67	-14.72	-11.73	-6.51	12.06	-1.72
3	-7.72	0.82	-9.89	-10.63	-6.40	10.87	-1.57
4	-6.99	1.47	-10.42	-10.87	-5.39	10.79	-1.52
5	-6.86	1.15	-9.88	-10.10	-6.32	11.02	-1.45
3j6g	-9.66	-	-	-12.85	-7.1	12.44	-2.15
5syf	-9.57	-	-	-12.79	-9.19	14.26	-1.86
6ew0	-8.76	-	-	-14.31	-5.19	12.93	-2.19

Table S4. Statistical significance test (p-values of the independent samples T-test calculated using the *ttest_ind()* function of SciPy) for distributions of the total paclitaxel-tubulin interaction energy in different clusters.

		Clusters				
		1	***2***	***3***	***4***	***5***
Clusters	***1***		$< 10^{-308}$	$< 10^{-308}$	$< 10^{-308}$	$< 10^{-308}$
	2			0.00130	$2.33 \cdot 10^{-97}$	$4.13 \cdot 10^{-71}$
	3				$1.34 \cdot 10^{-48}$	$3.15 \cdot 10^{-76}$
	4					0.00194

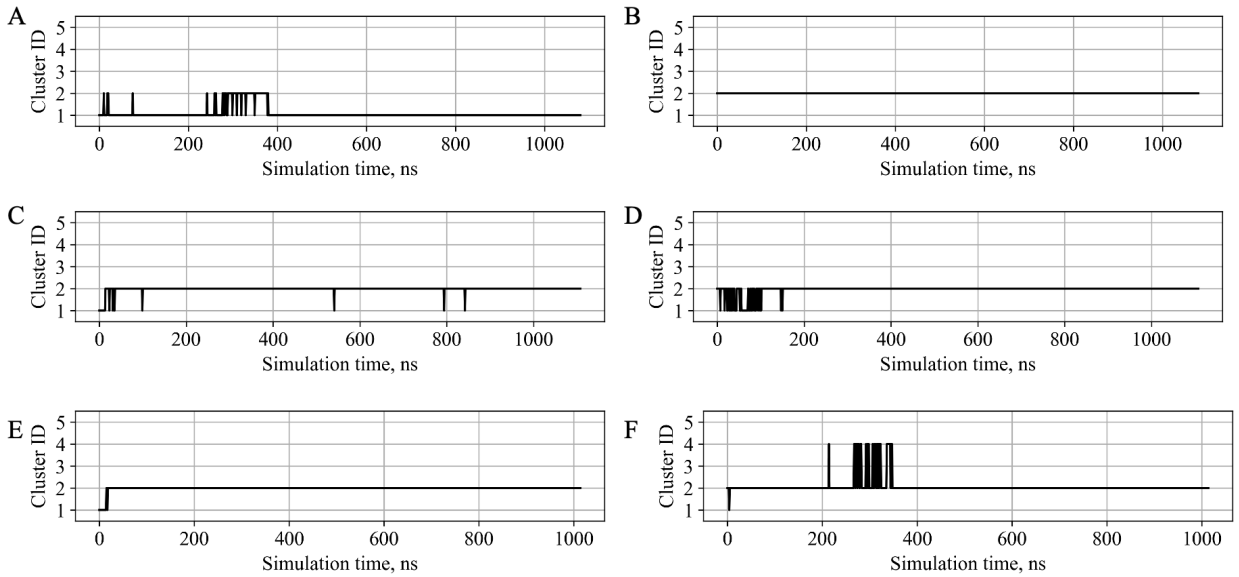

Figure S3. Transitions between the clusters observed in two monomers of β-tubulin comprising the simulated protofilament based on the experimental structure with the PDB code 3j6g in three replicated trajectories (A-B, C-D, and E-F).

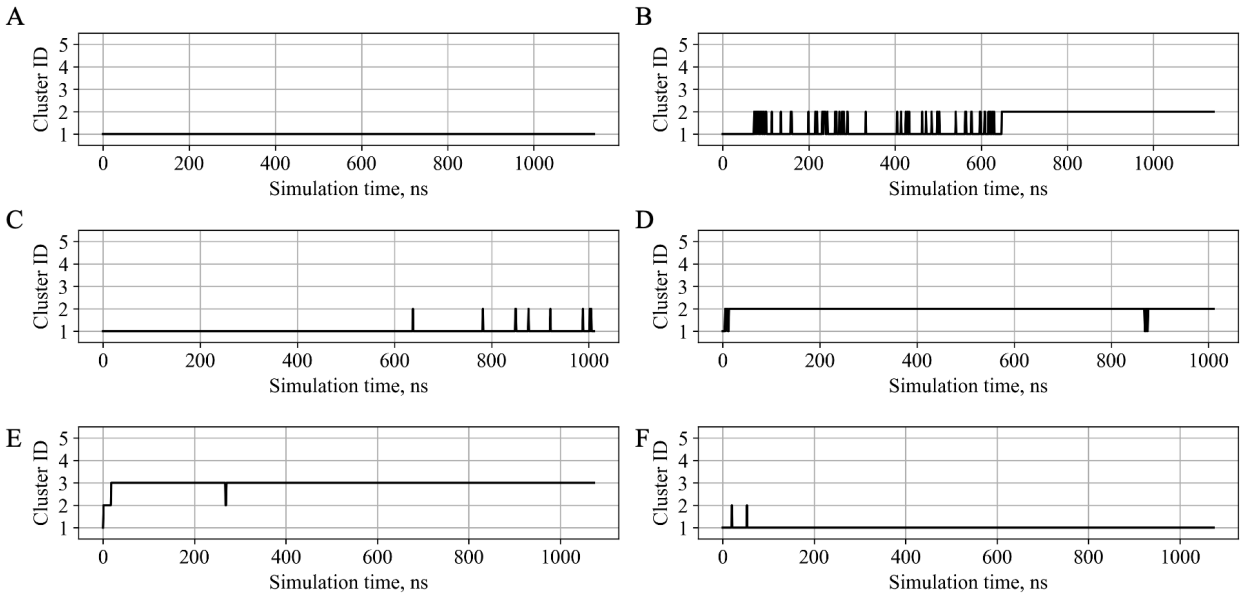

Figure S4. Transitions between the clusters observed in two monomers of β-tubulin comprising the simulated protofilament based on the experimental structure with the PDB code 5syf in three replicated trajectories (A-B, C-D, and E-F).

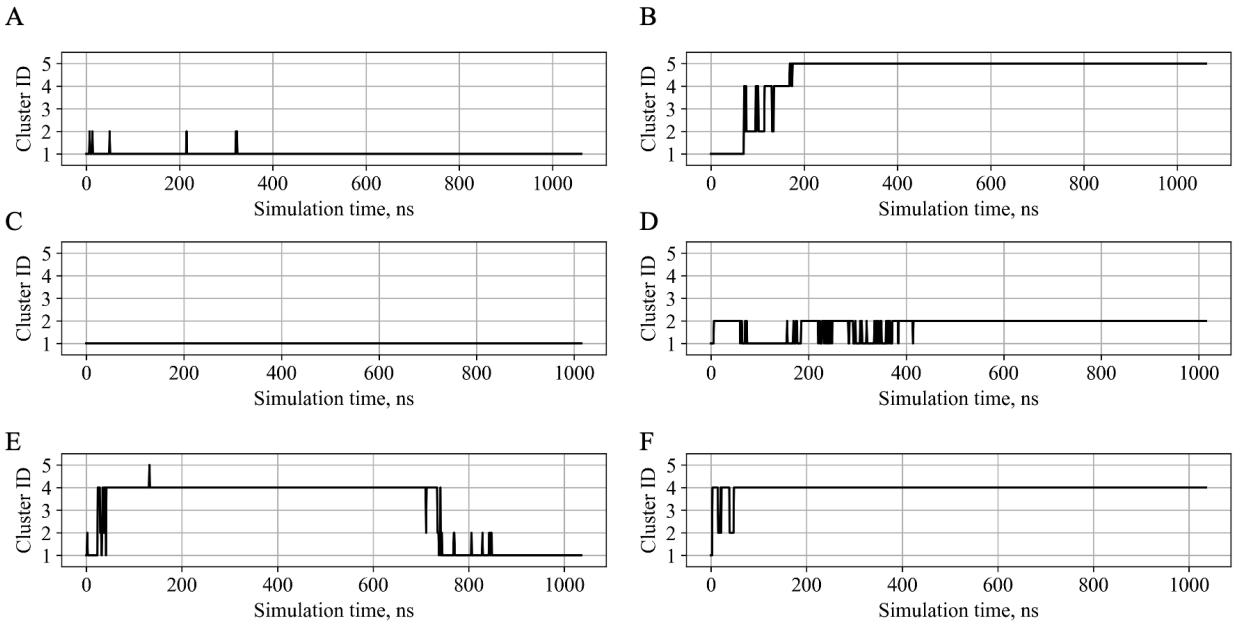

Figure S5. Transitions between the clusters observed in two monomers of β-tubulin comprising the simulated protofilament based on the experimental structure with the PDB code 6ew0 in three replicated trajectories (A-B, C-D, and E-F).

Table S5. Hydrogen bonds between paclitaxel and the protein, which exist for at least 1% of the total simulation time.

Acceptor	***Donor***	***Lifetime (fraction of the total simulation time)***
Paclitaxel (1OEE, OC6)	Arg 276 (NE, NH1, NH2)	0.159
Gln 279 (O)	Paclitaxel (OD5)	0.192
Paclitaxel (3OD2)	Thr 274 (HN)	0.308
Paclitaxel (1OBB)	His 227 (HE2)	0.551
Paclitaxel (1OI4)	Gly 277 (HN)	0.041
Paclitaxel (OI2, OD5)	Gln 280 (NE2)	0.042
Paclitaxel (OAA)	Arg 359 (NE, NH1, NH2)	0.011

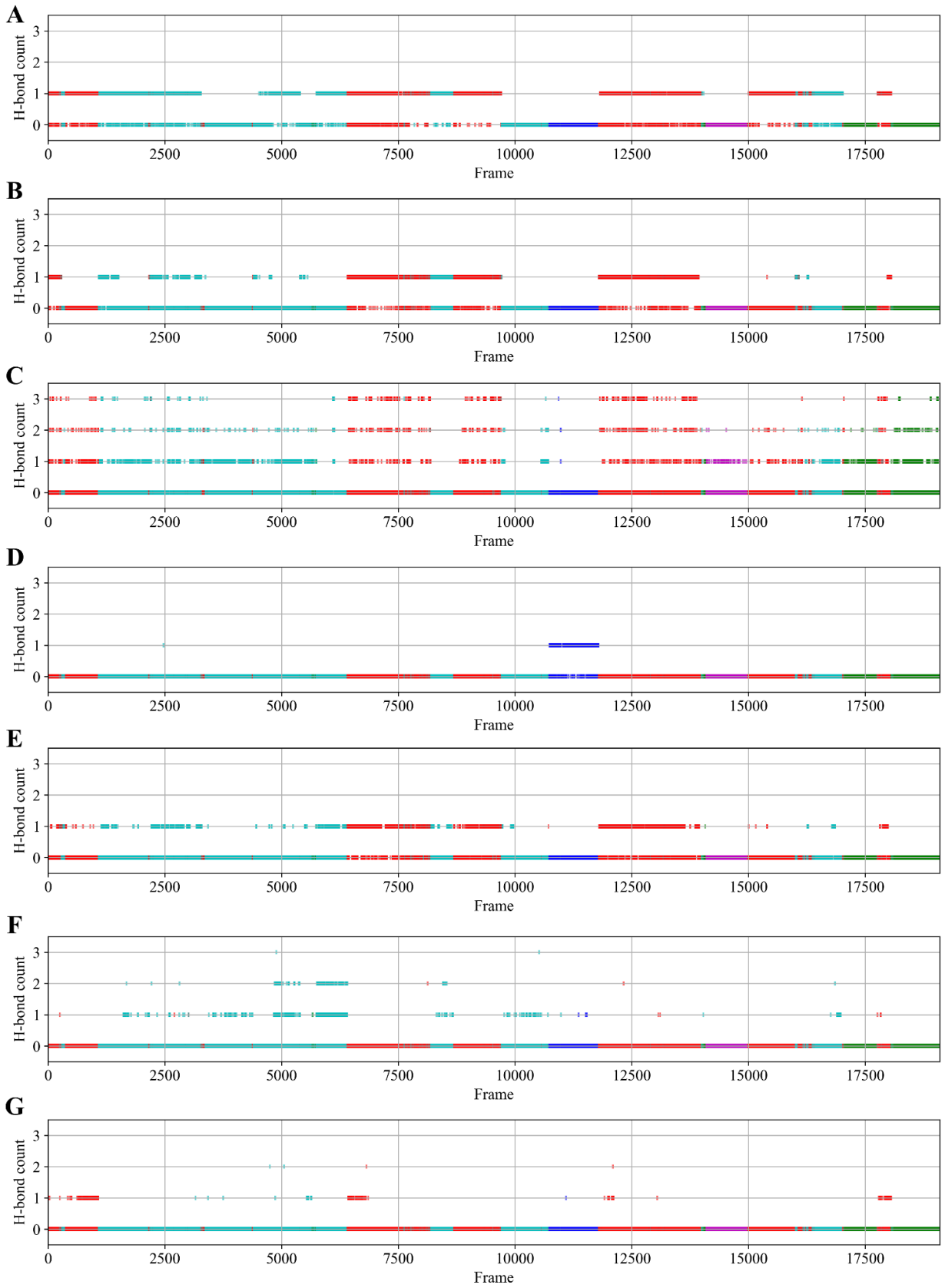
A
B
C
D
E
F
G
H-bond count
Frame
0
1
2
3
0
2500
5000
7500
10000
12500
15000
17500

Figure S6. Population of hydrogen bonds between paclitaxel and the protein throughout the simulations. **A**: His 227; **B**: The 274; **C**: Arg 276; **D**: Gly 277; **E**: Gln 279; F: Gln 280; G: Arg 359. Colors correspond to the determined clusters of structures.

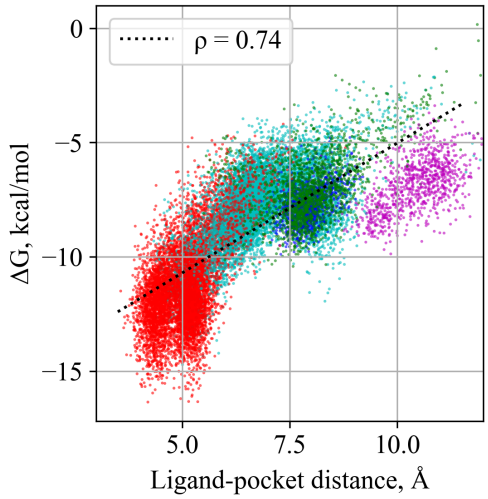

Figure S7. Relations of the free energy of paclitaxel binding to the ligand-binding site distance. The binding free energy of paclitaxel plotted against the ligand-binding site distance for all the analyzed conformations (colors correspond to the determined clusters of structures).

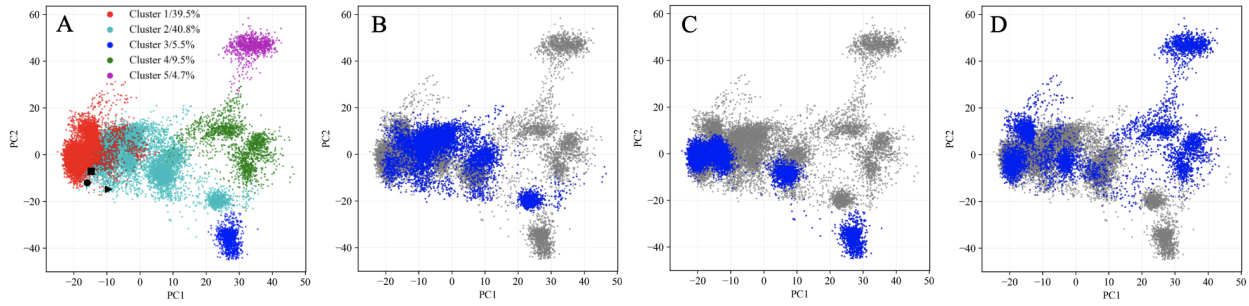

Figure S8. Conformational space of paclitaxel with its neighboring residues explored in the three series of conducted simulations starting from different experimental structures (PDB codes 3j6g, 5syf, and 6ew0). **A**: Projection of conformations of the pacitaxel binding pocket observed in all series of molecular dynamics simulations onto the two top principal components. Each dot represents a single conformation of paclitaxel with its local amino acid environment. Different colors stand for six identified clusters of conformations; **B-D**: conformations observed in the simulations starting from 3j6g (**B**), 5syf (**C**), and 6ew0 (**D**) experimental structures (shown in blue, the complete conformational space is shown in gray as a reference).

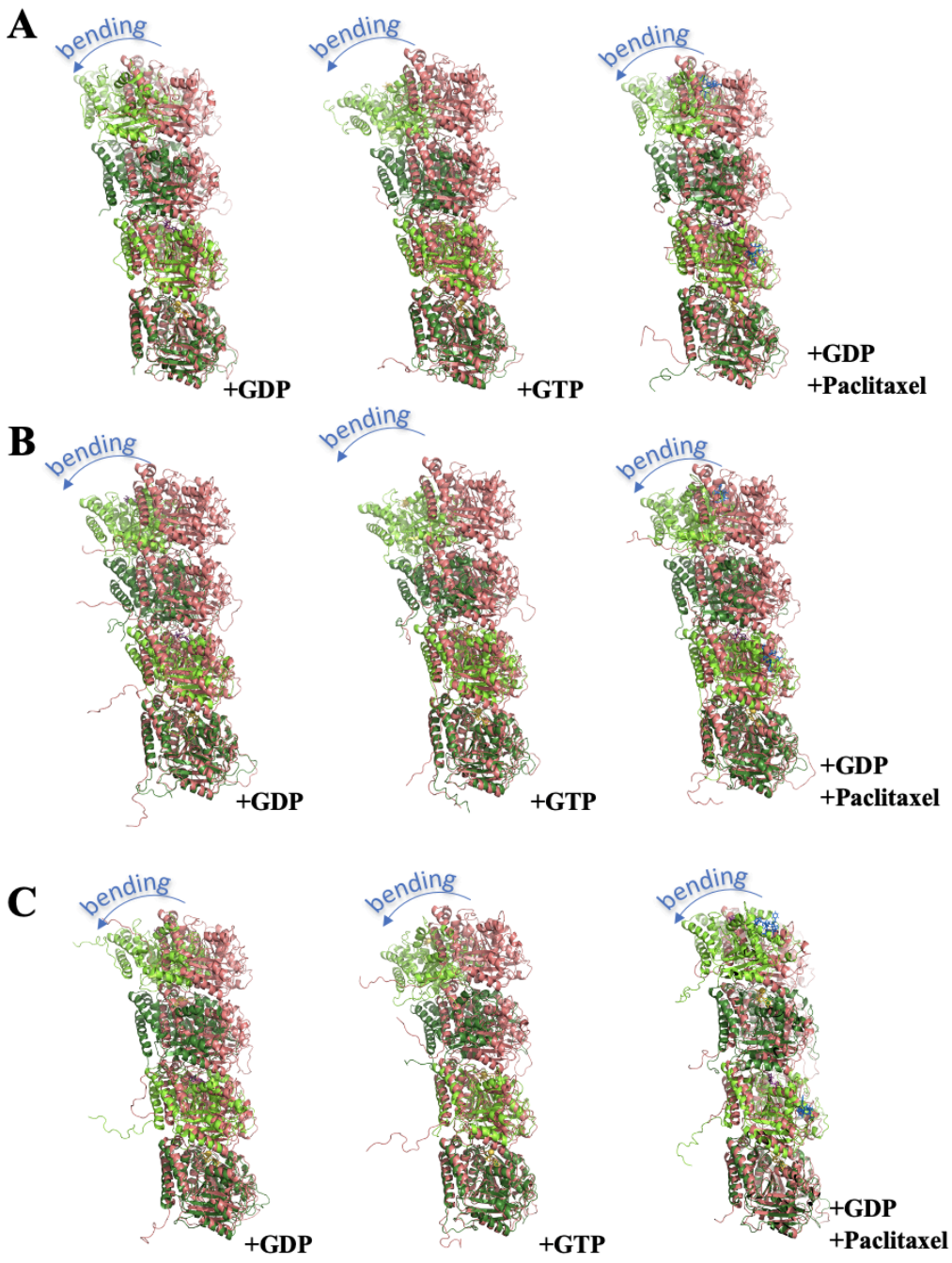

Figure S9. Bending of the model tetrameric GDP-bound, GTP-bound, and paclitaxel bound protofilaments. Representative snapshots from the unrestrained simulations are shown aligned by the bottom monomer with the initial "straight" structures. A: 6dpv, 6dpu, and 5syf; B: 6evz, 6evw, and 6ew0; C: 3j6f, 3j6e, and 3j6g structures. The simulations for the paclitaxel-bound systems (5syf, 6ew0, and 3j6g) are reported in the present study; the simulations for 3j6f and 3j6e are were reported earlier [2]; data for 6dpv, 6dpu, 6evz, and 6evw are not yet published.

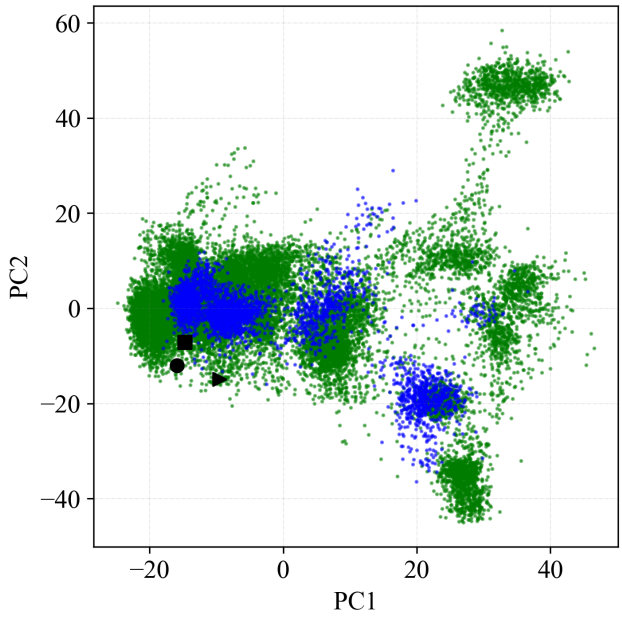

Figure S10. Conformational space of paclitaxel with its neighboring residues explored in the simulations conducted with the positional restraints applied to the tubulin protofilaments (in green) and in the unrestrained simulations (in green) projected onto the two top principal components (calculated solely for the unrestrained simulations).

Table S6. Residues, which contribute over ±0.5 kcal/mol to the total binding free energy in each of 5 identified clusters of conformations. All values are in kcal/mol.

Cluster 1		***Cluster 2***		***Cluster 3***		***Cluster 4***		***Cluster 5***	
Residue	***Energy***	***Residue***	***Energy***	***Residue***	***Energy***	***Residue***	***Energy***	***Residue***	***Energy***
VAL23	-1.08	THR214	-1.34	VAL23	-0.56	VAL23	-0.59	LEU215	-2.94
GLU27	0.9	LEU215	-0.54	GLU27	0.52	LEU215	-1.3	LYS216	-1.01
LEU215	-1.53	ASN226	-1.23	LEU215	-0.88	LEU217	-0.94	LEU217	-1.53
LEU217	-0.51	HIS227	-1.06	HIS227	-2.09	ASP224	0.67	ASP224	1.11
ASP224	0.67	SER230	-0.91	ALA231	-1.23	HIS227	-1.65	HIS227	-1.9
HIS227	-1.73	ALA231	-0.54	PHE270	-0.88	LEU228	-0.77	LEU228	-0.9
LEU228	-0.92	PRO272	-0.99	SER275	-1.83	ALA231	-0.8	SER275	-1.55
SER230	-0.58	LEU273	-0.62	ARG276	-0.96	ARG276	-1.85	ARG276	-2.28
ALA231	-1.04	SER275	-1.09	GLY277	-0.65	GLN279	-1.59		
PHE270	-1.18	SER278	-0.91	PRO358	-0.5	LEU361	-1.48		

PRO272	-0.78	GLN279	-0.71	ARG359	-0.61				
LEU273	-1.9	PRO358	-0.76	GLY360	-1.32				
THR274	-1.14	ARG359	-0.52	LEU361	-2.59				
ARG276	-1.13	GLY360	-1.25						
GLN279	-0.9	LEU361	-0.75						
ARG318	-0.78								
PRO358	-0.89								
ARG359	-1.18								
GLY360	-0.73								
LEU361	-2.25								

Table S7. Membership of key amino acids contributing to paclitaxel binding over ±0.5 kcal/mol in the identified clusters 1-5.

Clusters	***Count***	***Residues***
cluster 1 cluster 2 cluster 3 cluster 4 cluster 5	2	HIS227 LEU215
cluster 1 cluster 2 cluster 3 cluster 4	2	ALA231 LEU361
cluster 1 cluster 3 cluster 4 cluster 5	1	ARG276
cluster 1 cluster 2 cluster 3	3	PRO358 ARG359 GLY360
cluster 1 cluster 2 cluster 4	1	GLN279
cluster 1 cluster 3 cluster 4	1	VAL23
cluster 1 cluster 4 cluster 5	3	ASP224 LEU217 LEU228
cluster 2 cluster 3 cluster 5	1	SER275
cluster 1 cluster 2	3	LEU273 PRO272 SER230
cluster 1 cluster 3	2	PHE270 GLU27
cluster 1	2	THR274 ARG318
cluster 2	3	SER278 THR214 ASN226
cluster 3	1	GLY277
cluster 5	1	LYS216

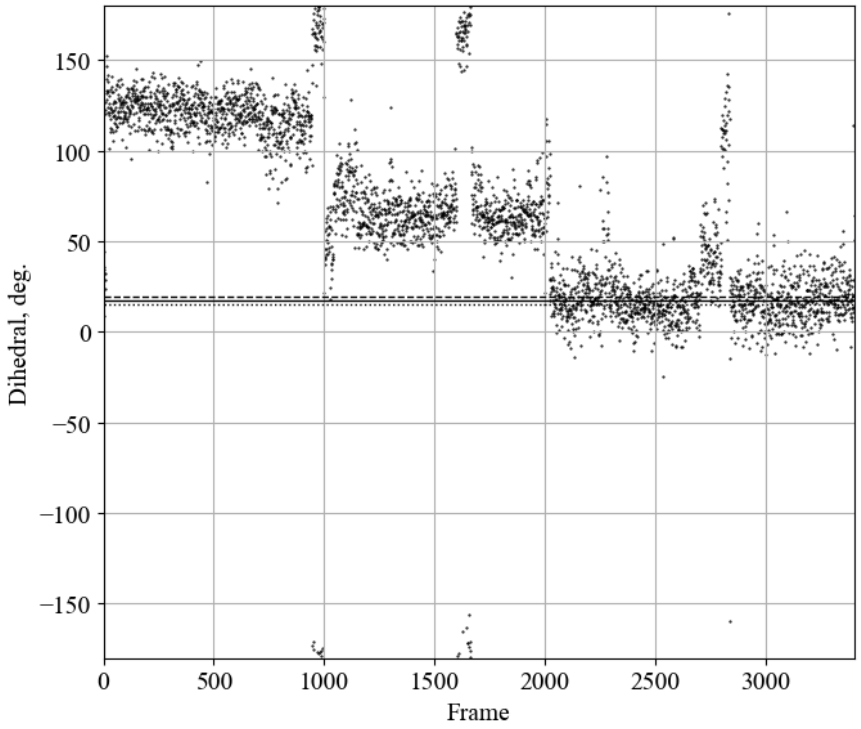

Figure S11. Dihedral values for the bond connecting the tetracyclic and benzylbenzamide moieties of paclitaxel throughout the simulations of the restrained "straight" protofilaments. Dashed lines correspond to the values observed in the experimental structures.

Table S8. Comparison of the key amino acids revealed in the present study and in previous computational studies by Xu et al. [3], Churchill et al. [4] and Prota et al. [5] as well as the experimentally determined mutations causing paclitaxel resistance. Residue numbers are given for *Sus scrofa* (3j6g structure) and *Bos taurus* (1jff structure, in brackets).

Present study (> 0.5 kcal/mol)	Xu et al., 2012 (ΔG, kcal/mol)	Churchill et al., 2015 (ΔG, kcal/mol)	Prota et al., 2023 (> 1 kcal/mol)	Experimental resistance mutations
Val 23 (23)		-4.92	+	V23T [6]
Glu 27 (27)	-4.04		+	
Thr 214 (216)		-1.77		
Leu 215 (217)		-2.96	+	L215I [7]
Lys 216 (218)	-8.08			
Leu 217 (219)				L217R [7]
Asp 224 (226)	-9.66	-1.24	+	

Asn 226 (228)				
His 227 (229)	-3.80	-4.09	+	H227N [6]
Leu 228 (230)		-1.82	+	L228F/R [7]
Ser 230 (232)				
Ala 231 (233)	0.86	-2.18	+	A231T [8]
Phe 270 (272)		-1.89	+	F270V [9]
Pro 272 (274)		-2.20	+	
Leu 273 (275)	-1.34	-3.92	+	
Thr 274 (276)	-7.80	-0.96	+	T274I [10]
Ser 275 (277)	-4.47			
Arg 276 (278)	-6.74		+	
Gly 277 (279)	-1.96			
Ser 278 (280)				
Glu 279 (281)			+	
Arg 318 (320)	-3.51			
Pro 358 (360)		-2.58	+	
Arg 359 (369)	-0.93	-7.00	+	
Gly 360 (370)	-0.50	-1.89	+	
Leu 361 (371)	-4.04	-3.47	+	

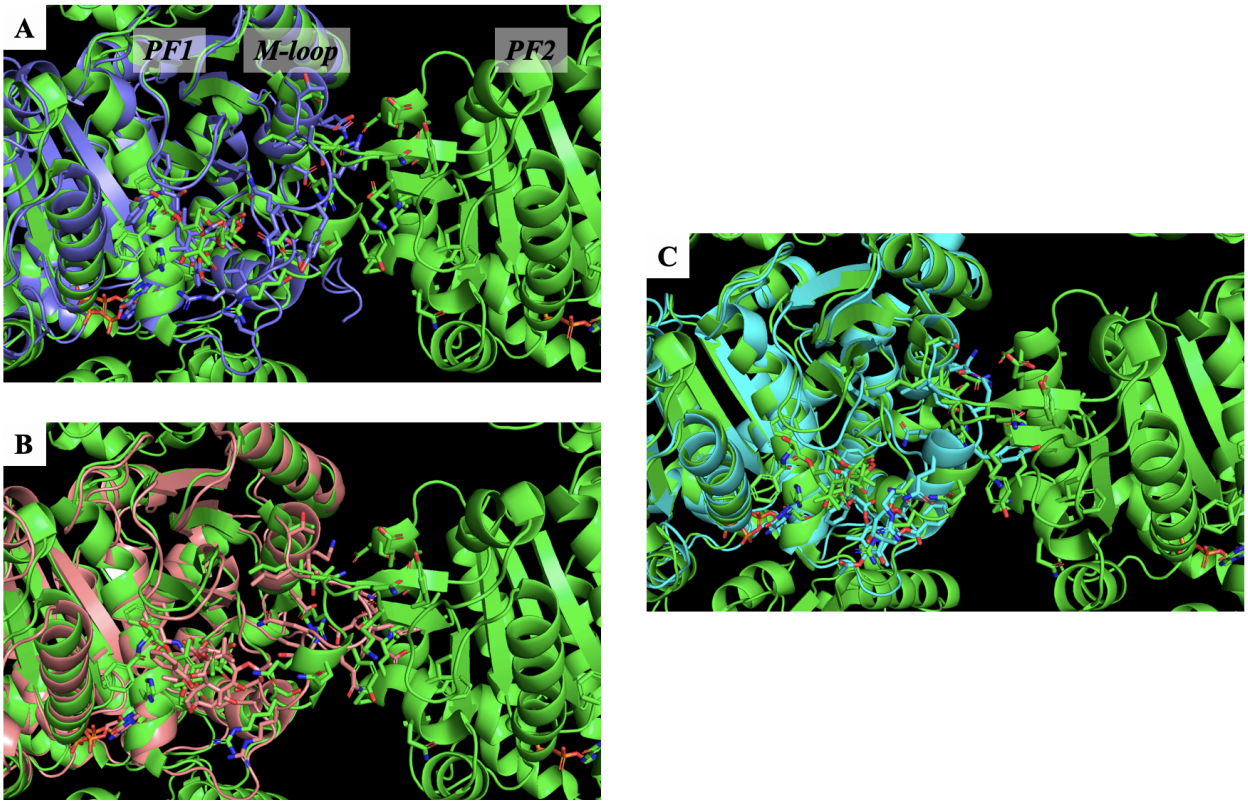

Figure S12. Alignments of the representative β-tubulin structures of cluster 1 (**A**, blue), 3 (**B**, red), and 5 (**C**, cyan) onto the structure of the complete microtubule (PDB code 3j6g, green). The residues of M-loop and the regions in its vicinity at the interface between the neighboring protofilaments are shown using the stick representation.

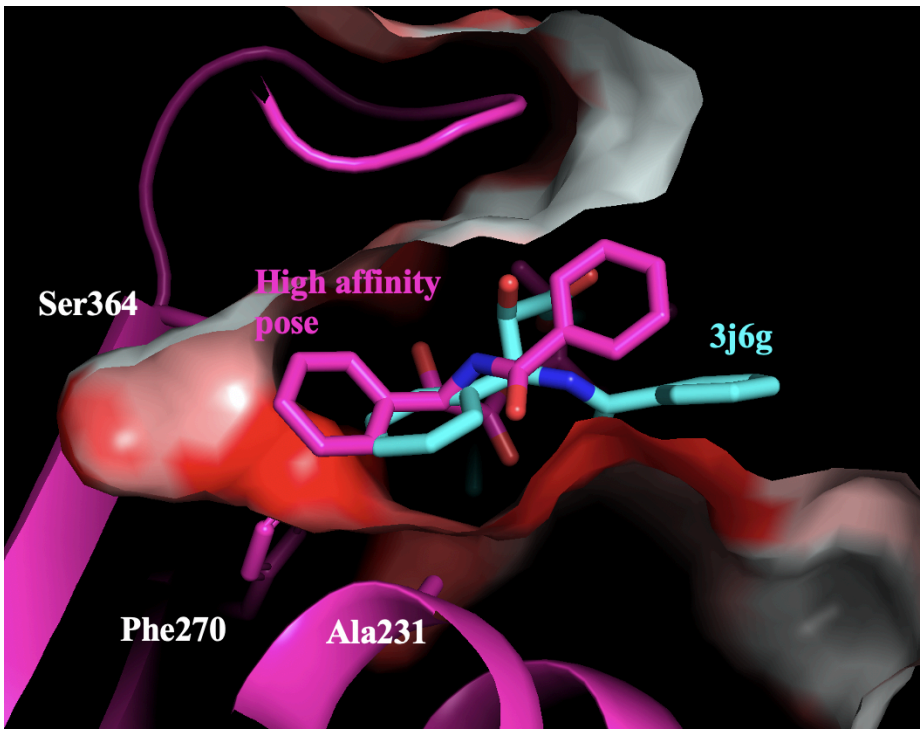

Figure S13. The cavity formed by the B9-B10 loop and H1 helix with the high-affinity conformation of paclitaxel stuck into it. Position of paclitaxel in the aligned initial experimental model (with PDB code 3j6g) is shown for comparison. The surface is cut in order to show the ligand.

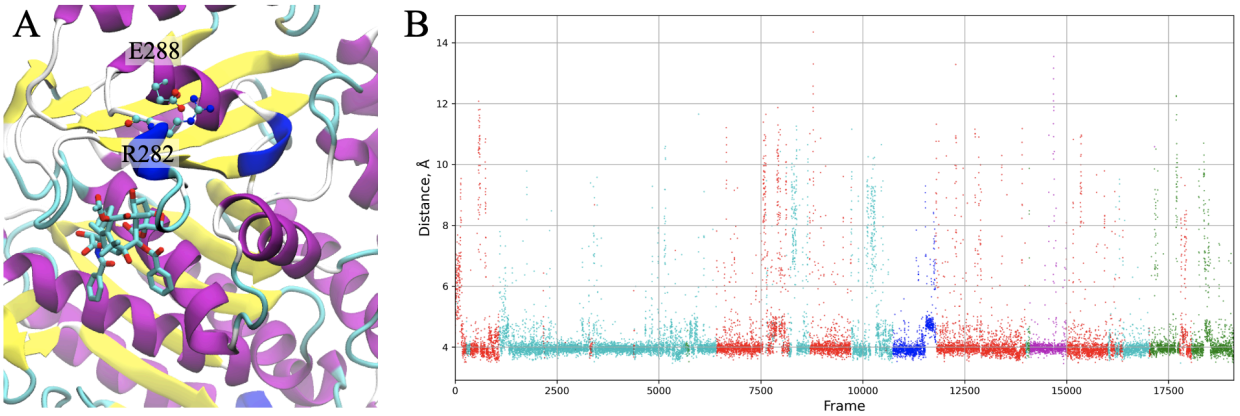

Figure S14. A: The salt bridge between R282 of the M-loop and E288 in β-tubulin. B: the distance between CZ of R282 and CD of E288 as a function of the simulation time. Colors indicate the clusters of conformations.

Table S9. Details of performed molecular dynamics simulations.

System	***Simulation time, μs***	***Number of atoms***	***Simulation box, nm × nm × nm***
3j6g tetramer, unrestrained	1.08, 1.11, 1.01	283248	10.7 x 11.9 x 22.5
5syf tetramer, unrestrained	1.14, 1.01, 1.07	307453	11.3 x 12.5 x 22.2
6ew0 tetramer, unrestrained	1.06, 1.02, 1.04	346257	12.3 x 12.8 x 22.4
5syf tetramer, restrained	1.0, 0.7	307453	11.3 x 12.5 x 22.2

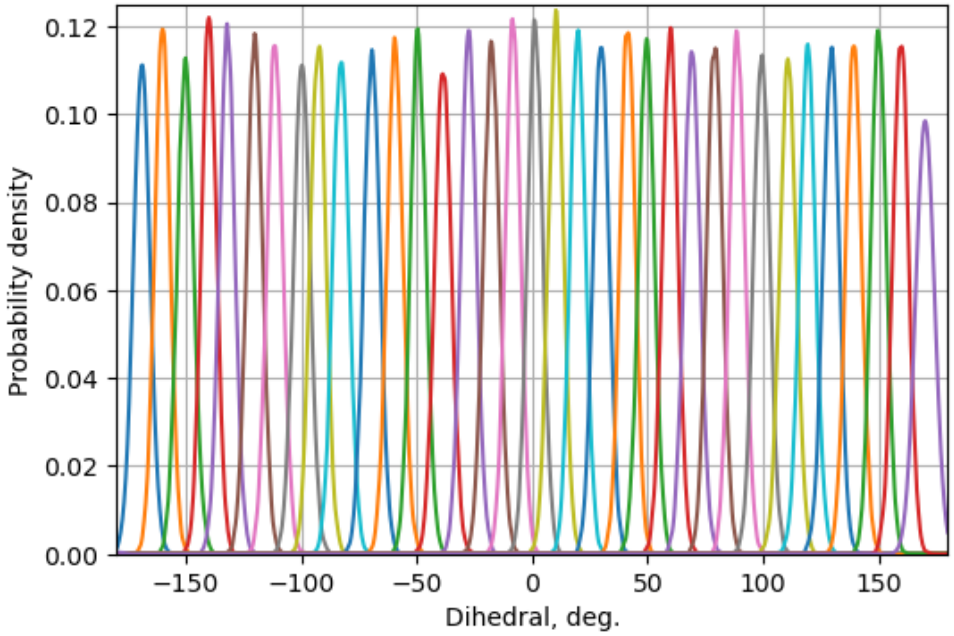

Figure S15. Probability densities of a dihedral corresponding to the rotation around a bond connecting the tetracyclic and benzylbenzamide moieties of paclitaxel for the different umbrella sampling windows.

Table S10. Full list of residues (86 residues) considered in the paclitaxel binding site (at least in one of the initial experimental structures чor simulation frames, the distance between paclitaxel and at least one heavy atom of a residue did not exceed 7 Å).

Ile 16	Glu 27	Phe 212	Gly 223	Met 233	Phe 270	Gln 280	Val 316	Lys 362
Ala 18	His 28	Arg 213	Asp 224	Ser 234	Ala 271	Tyr 281	Phe 317	Met 363
Lys 19	Gly 29	Thr 214	Leu 225	Gly 235	Pro 272	Arg 282	Arg 318	Ser 364
Phe 20	Gln 43	Leu 215	Asn 226	Val 236	Leu 273	Ala 283	Gly 319	Ala 365
Trp 21	Pro 80	Lys 216	His 227	Thr 237	Thr 274	Leu 284	Ile 356	Thr 366
Glu 22	Phe 81	Leu 217	Leu 228	Thr 238	Ser 275	Leu 289	Pro 357	Phe 367
Val 23	Leu 207	Thr 218	Val 229	Cys 239	Arg 276	Gln 292	Pro 358	
Ile 24	Tyr 208	Thr 219	Ser 230	Arg 241	Gly 277	Lys 297	Arg 359	
Ser 25	Ile 210	Pro 220	Ala 231	Phe 242	Ser 278	Asn 298	Gly 360	
Asp 26	Cys 211	Thr 221	Thr 232	Gly 269	Gln 279	Met 300	Leu 361	

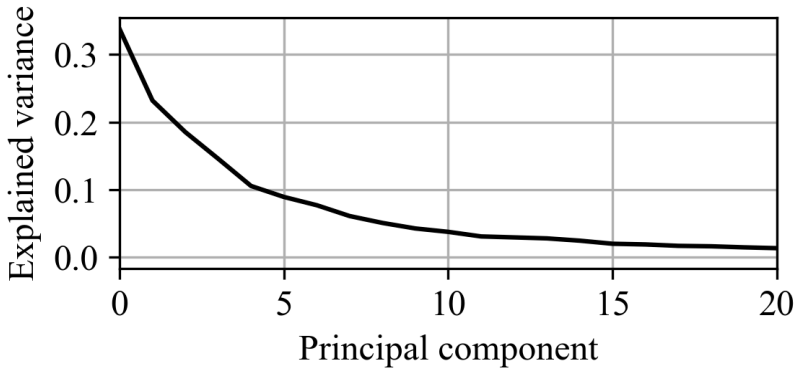

Figure S16. Fraction of the total variance in the trajectory dataset explained by top 15 principal components.

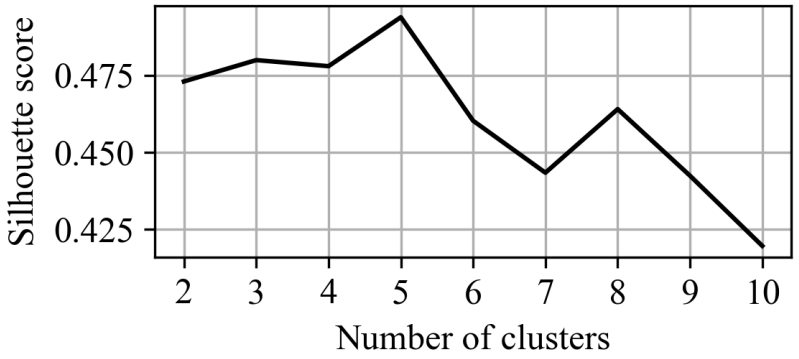

Figure S17. Silhouette score for different numbers of clusters identified by means of agglomerative clustering.

References

1. Sehnal, D. *et al.* Mol* Viewer: modern web app for 3D visualization and analysis of large biomolecular structures. *Nucleic Acids Res.* **49**, W431–W437 (2021).

2. Fedorov, V. A. *et al.* Mechanical properties of tubulin intra- and inter-dimer interfaces and their implications for microtubule dynamic instability. *PLoS Comput. Biol.* **15**, e1007327 (2019).

3. Xu, S. *et al.* Molecular dynamics simulation and density functional theory studies on the active pocket for the binding of paclitaxel to tubulin. *J. Mol. Model.* **18**, 377–391 (2012).

4. Churchill, C. D. M., Klobukowski, M. & Tuszynski, J. A. Elucidating the mechanism of action of the clinically approved taxanes: a comprehensive comparison of local and allosteric effects. *Chem. Biol. Drug Des.* **86**, 1253–1266 (2015).
5. Prota, A. E. *et al.* Structural insight into the stabilization of microtubules by taxanes. *Elife* **12**, (2023).
6. Dostál, V. & Libusová, L. Microtubule drugs: action, selectivity, and resistance across the kingdoms of life. *Protoplasma* **251**, 991–1005 (2014).
7. Gonzalez-Garay, M. L., Chang, L., Blade, K., Menick, D. R. & Cabral, F. A beta-tubulin leucine cluster involved in microtubule assembly and paclitaxel resistance. *J. Biol. Chem.* **274**, 23875–23882 (1999).
8. Verrills, N. M. *et al.* Microtubule alterations and mutations induced by desoxyepothilone B: implications for drug-target interactions. *Chem. Biol.* **10**, 597–607 (2003).
9. Giannakakou, P. *et al.* Paclitaxel-resistant human ovarian cancer cells have mutant beta-tubulins that exhibit impaired paclitaxel-driven polymerization. *J. Biol. Chem.* **272**, 17118–17125 (1997).
10. Giannakakou, P. *et al.* A common pharmacophore for epothilone and taxanes: molecular basis for drug resistance conferred by tubulin mutations in human cancer cells. *Proc. Natl. Acad. Sci. U. S. A.* **97**, 2904–2909 (2000).